Available online at www.sciencedirect.com
ScienceDirect
Trans. Nonferrous Met. Soc. China 32(2022) 45−63
Transactions of Nonferrous Metals Society of China
www.tnmsc.cn

Structural transformation and energy analysis for pile-up dislocations at triple junction of grain boundary

Ying-jun GAO[1], Zong-ji HUANG[1], Qian-qian DENG[1], Kun LIAO[1], Yi-xuan LI[1], Xiao-Ai YI[1], Zhi-rong LUO[2]

1. Guangxi Key Laboratory of Advanced Energy Materials, Guangxi Key Laboratory for the Relativistic Astrophysics, School of Physics Science and Engineering, Guangxi University, Nanning 530004, China;
2. School of Physics and Telecommunication Engineering, Yulin Normal University, Yulin 537000, China

Received 19 January 2021; accepted 23 July 2021

Abstract: An energy model for the structure transformation of pile-ups of grain boundary dislocations (GBD) at the triple-junction of the grain boundary of ultrafine-grain materials was proposed. The energy of the pile-up of the GBD in the system was calculated by the energy model, the critical geometric and mechanical conditions for the structure transformation of head dislocation of the pile-up were analyzed, and the influence of the number density of the dislocations and the angle between Burgers vectors of two decomposed dislocations on the transformation mode of head dislocation was discussed. The results show when the GBD is accumulated at triple junction, the head dislocation of the GBD is decomposed into two Burgers vectors of these dislocations unless the angle between the two vectors is less than 90°, and the increase of applied external stress can reduce the energy barrier of the dislocation decomposition. The mechanism that the ultrafine-grained metal material has both high strength and plasticity owing to the structure transformation of the pile-up of the GBD at the triple junction of the grain boundary is revealed.

Key words: triple junction of grain boundary; dislocation pile-up; dislocation structural transformation; energy model for pile-up; ultrafine-grain materials

1 Introduction

Ultrafine-grained metal materials usually exhibit high strength [1] but poor plasticity. It is reported that ductility occurs in some specific nanocrystalline structural materials under mechanical loading [2]. For example, good plasticity is exhibited in some ultrafine-grained alloys at relatively high strain rate and low temperature [3], which indicates high flow stress and strong ductility, i.e., both good plasticity and high strength can be obtained for special ultrafine-grained alloys. The structure and property in the solids are strongly affected by dislocation structural transformation of the grain boundaries (GB) [4], especially due to the higher volume fraction of the triple junction in the ultrafine-grained materials and nanocrystalline structural materials. Therefore, the structure of the grain boundary dislocations (GBD) and triple junctions of the GB play an important role in the excellent mechanical properties of ultrafine-grained and nanocrystalline materials. Generally, there are large number of the GBDs during the production of polycrystalline materials [5]. On the asymmestric tilt GB, there is an angle between Burgers vectors of the arranged dislocations of the GB, whose vectors can be regarded as one portion of Burgers vector perpendicular to the GB and one portion of Burgers vector parallel to the GB [6]. Under loading of the external stress, the dislocation with Burgers vector parallel to the GB in the metals will move along the direction of the GB. At present, it is

Corresponding author: Ying-jun GAO, Tel: +86-13877832545, E-mail: gaoyj@gxu.edu.cn
DOI: 10.1016/S1003-6326(21)65777-1

clear that GB slipping and dislocation moving dominate the deformation behavior of polycrystalline materials [7]. It is generally believed that GB slipping is regarded as a motion of the GBD along the plane of the GB [8]. Under the action of shear stress, the GBD with the Burgers vector parallel to the GB can slip along the GB [9]. When encountering the bend of the GB, the GBD will stay at the triple junction [10]. The GBD is blocked at the triple junction and dislocations are piled up [11,12]. A large number of GBDs are blocked at the triple junction to lead to stress concentration, which can cause structural transformation of the pile-up [13] of the GBD at triple junction to emit dislocation moving along another GB, or to induce microcrack nucleation to release stress and strain energy [14,15], or to cause the formation of nanovoids at the triple junction [16]. There are different forms and reaction mechanisms of the dislocation when the GBD are blocked at triple junction, which lead to different effects and different properties of the material [17−21]. For example, the dislocation pile-up formed by one row of the GBDs staying at triple junction [22,23], or gathered by two row of the GBD at triple junction [24] under deformation, will cause different types of reaction modes [25] of the dislocations at triple junction. There are a few transformation modes [6,10,26] of the GBD. For example, head dislocation of GBD at triple junction is decomposed into two mobile dislocations which move along the other two GB at triple junction without the strengthening effect of the dislocation. Experimental observations [27] have found that the merging of immobile dislocations can occur at the triple junction with the strengthening effect, accompanied by emitting a movable dislocation which plays a softening role. The GBD can be decomposed and transformed into two new dislocations, and one of the new dislocations is an immobile dislocation staying at triple junction, while the other new dislocation moves into grain or moves along another adjacent grain boundary [6,28]. Such dislocation reactions repeat many times in a certain range of energy conditions, and result in more and more immobile dislocations accumulating at triple junction to form a larger dislocation with larger Burgers vectors [6,18], which directly influences on the mode of the deformation in nanocrystalline metals [29,30] and on the characteristics of strengthening, softening and fracture in the fine-grained alloy [31].

Many theoretical models of the dislocation pile-ups were studied and reported [17,23,31−37], but the role of the structure transformation of the pile-ups of the GBD at triple junction of the GB during plastic deformation in polycrystalline materials is still not clear. The reason is that it is difficult to distinguish different effects between the triple junction and the conventional grain boundary in the experiment [33,36]. In this case, constructing the theoretical model of the GBD transformation at triple junction is of great significance [35,38] to understand the relationship between the structural transition of the dislocation pile-ups of the triple junction and the properties of strength and ductility in ultrafine-grain. Before this research, the authors have studied the motion of the blocked and decomposed GBD [25,26,39,40] under loading. The main purpose of this work is to propose a phenomenological energy model for the decomposition of the GBD with one immobile dislocation at triple junction and one mobile dislocation moving along another GB, to calculate the systematic energy variation of the structure transformation of the blocked GBD under an external stress. We analyze the critical geometric and mechanical conditions of the decomposition reaction of the head dislocations, and discuss the influence of the density of blocked dislocations and the angle of two Burgers vectors of the decomposed dislocations on the transformation mode of the head dislocation. Finally, we reveal the dislocation mechanism of strengthening and softening of the ultrafine-grain structural materials, and point out new useful guidance to improve the plasticity of ultrafine-grained metal materials

2 Phenomenological model of dislocation transformation

The accumulated dislocations at triple junction are required for the strengthening and hardening, while the motion of the GBD and the release of the strain energy are required for the softening at the triple junction, in which it can accommodate the larger plastic deformation. The immobile dislocation plays a strengthening role, while the accompanying mobile dislocation can enhance the toughness. Therefore, we only consider the case

where one decomposed dislocation can be accommodated at the triple-junction of GB, and the other can be movable along the other GB, as shown in Figs. 1(a−c). Here the three GB joined at triple junction are assumed to be straight. Due to the bending of the GBs at triple junction, the head dislocation b stops moving at it. The GBD at triple junction are taken in account. The first blocked dislocation, i.e., head dislocation, decomposes and transforms into two new dislocations because of the stress concentration at the triple junction. The two new dislocations are written as b_{1a} and b_{1b}. The dislocation b_{1a} moves along the one of adjacent GB, where the angle between the direction of the GB and that of original GB is α_1. The other dislocation is an immovable dislocation, which stays at triple junction, and the angle between the direction of Burgers vector of the immovable dislocation and the original GB is α_2. This transition process can be considered as the following three states, corresponding to the dislocation configuration of Figs. 1(a, b, c), respectively. According to the configuration of these three dislocation structures, the energy representation of the system can be written.

2.1 System energy before GBD decomposition

As shown in Fig. 1(a), a dislocation pile-up at local triple junction in polycrystalline materials is given. Under the action of external stress, due to the moving of the horizontal grain boundary, the head dislocation of GBD moving is started, and it is assumed that there are n dislocations (dislocation b_1, b_2, ⋯, b_n arranged in the GB) piling up along the GB and blocked at triple junction. At present, the energy of the system is E_1, and consists of three parts:

$$E_1=E'_{n-1}+E_b^s+E^{int} \tag{1}$$

where E'_{n-1} is the interaction between remaining $(n-1)$ GBD during the decomposition of the head dislocation. These $(n-1)$ GBD are regarded as a whole, and it can be approximately considered that E'_{n-1} remains unchanged during the wholes process. This part of energy is called the interaction energy of the residual GBD.

E_b^s is the self-energy of the head dislocation before the decomposition transition, and can be expressed as [6]

$$E_b^s=\frac{Gb^2}{4\pi(1-\nu)}\left(\ln\frac{R}{r_c}+z\right)=Db^2\left(\ln\frac{R}{r_c}+z\right) \tag{2}$$

where G is the shear modulus, $D=G/[4\pi(1-\nu)]$, R is shield length, r_c is the radius of the dislocation core, z is the energy parameter of the dislocation core, ν is Poisson ratio, b is the magnitude of Burgers vector.

E^{int} is the elastic interaction energy between

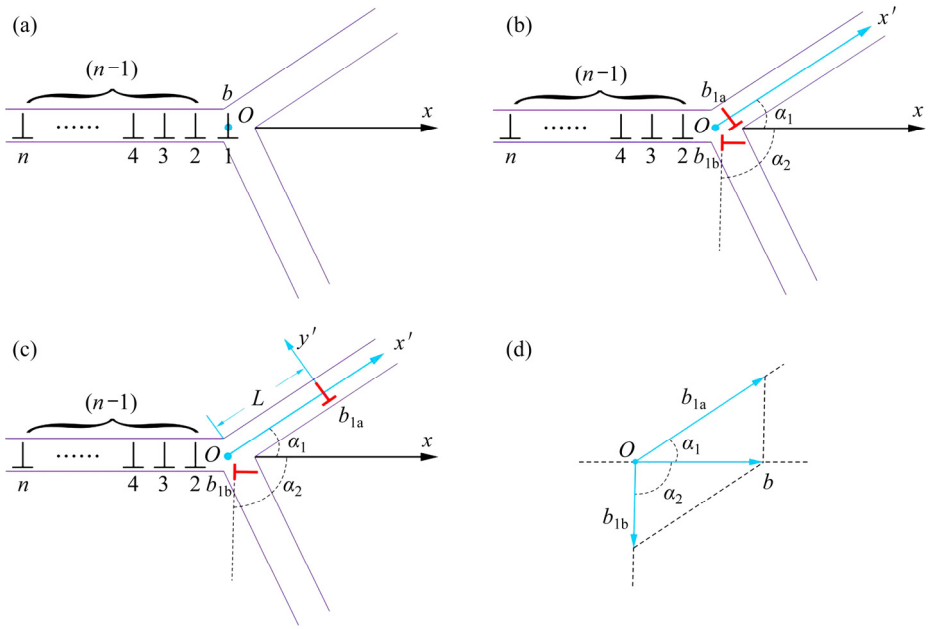

Fig. 1 Schematic diagram of transformation process of head dislocation: (a) GBD pile-up staying at triple junction; (b) Head dislocation decomposed into two new dislocations b_{1a} and b_{1b}; (c) One dislocation moving along adjacent GB, while another new dislocation staying at triple junction; (d) Geometric relationship between Burgers vectors of new dislocation and original dislocation at triple junction

the head dislocation and the unchanged (n−1) blocked GBD. It is assumed that the position of these (n−1) blocked GBD is fixed and does not change relatively. During the transformation of the head dislocation in the dislocation pile-up, because the new Burgers vector of the dislocation is generated in a certain range at triple junction, the above assumption is reasonable under such conditions. At this time, the interaction energy between these (n−1) blocked GBD can be written as [6]

$$E^{\text{int}}=Db^2\sum_{i=2}^{n}\ln\frac{R}{x_i} \tag{3}$$

where x_i is the distance between the ith GBD and the triple junction.

2.2 Decomposition of head dislocation of GBD

Under the action of the external stress and (n−1) blocked dislocation, the decomposition of the head dislocation b_1 occurs at triple junction, i.e., $b_1\rightarrow b_{1a}+ b_{1b}$, where b_{1b} is the immobile dislocation, and b_{1a} is the mobile dislocation, as shown in Fig. 1(b). The relationship between the amount of Burgers vectors of the head dislocation b_1 is shown in Fig. 1(d), and the new dislocation b_{1a} and b_{1b} can be written as

$$\begin{cases}b=b_{1a}\cos\alpha_1+b_{1b}\cos\alpha_2\\ b_{1a}\sin\alpha_1=b_{1b}\sin\alpha_2\end{cases} \tag{4}$$

where α_1 is the angle between the vector of b_{1a} and the horizontal x axis, while α_2 is the angle between the vector of b_{1b} and the horizontal x axis (as shown in Fig. 1(b)). In general, the b_{1a} and b_{1b} are not equal in magnitude. The smaller the α is, the larger the b_{1a} is.

2.3 System energy after GBD decomposition

After the decomposition transition of the head dislocation b_1 within the GBD at triple junction, the new dislocation b_{1b} stays at triple junction, while the other new dislocation b_{1a} moves along the adjacent grain boundary. It is assumed that the distance of new dislocation b_{1a} moving is L. The dislocation configuration of the system is shown in Fig. 1(c), and the energy is expressed as E_2, which can be written as

$$E_2=E'_{n-1}+E_{1a}^{\text{s}}+E_{1b}^{\text{s}}+E_{1a}^{\text{int}}+E_{1b}^{\text{int}}+E_{1a-1b}^{\text{int}}-A_{1a} \tag{5}$$

where E_{1a}^{s} (E_{1b}^{s}) is the self-energy of new dislocation b_{1a} (b_{1b}) decomposed by the head dislocation b_1, and the energy is satisfied with the following relation:

$$\frac{E_{1a}^{s}}{b_{1a}^2}=\frac{E_{1b}^{s}}{b_{1b}^2}=D\left(\ln\frac{R}{r_c}+z\right) \tag{6}$$

E_{1a}^{int} (E_{1b}^{int}) is the interaction energy between b_{1a} (b_{1b}) and whole of (n−1) blocked GBD, and it can be written as

$$E_{1a}^{\text{int}}=Dbb_{1a}\sum_{i=2}^{n}\psi(\alpha_1,x_{1ai},y_{1i}) \tag{7}$$

$$E_{1b}^{\text{int}}=Dbb_{1b}\sum_{i=2}^{n}\psi(\alpha_2,x_{1bi},y_{1bi}) \tag{8}$$

where $\psi(\alpha,x,y)=\dfrac{\cos\alpha}{2}\ln\dfrac{R^2}{x^2+y^2}-y\dfrac{x\sin\alpha+y\cos\alpha}{x^2+y^2}$, and is available in literature [6].

E_{1a-1b}^{int} is the elastic interaction energy between new dislocations b_{1a} and b_{1b}, and can be written as

$$E_{1a-1b}^{\text{int}}=Db_{1a}b_{1b}\sum_{i=2}^{n}\psi(\alpha_1+\alpha_2,x_0,y_0) \tag{9}$$

The distance that dislocation b_{1a} moves along the GB under external stress is L, as shown in Fig. 1(c). So, the work of the dislocation b_{1a} done by external stress is: $A_{1a}=\tau Lb_{1a}\cos\alpha_1$. Therefore, the difference between the energy E_2 after transformation and the energy E_1 before transformation can be expressed as

$$\begin{aligned}\Delta E=E_2-E_1=&\\ &D\{b_{1a}b_{1b}\psi(\alpha_1+\alpha_2,x_0,y_0)+\\ &b\sum_{i=2}^{n}\left[b_{1a}\psi(\alpha_{1a},x_{1ai},y_{1ai})+b_{1b}\psi(\alpha_{2a},x_{1bi},y_{1bi})-\right.\\ &\left.b\ln\left(\frac{R}{x_i}\right)\right]+\frac{D}{2}\left(b_{1a}^2+b_{1b}^2-b^2\right)\left(\ln\frac{R}{r_z}+Z\right)-\\ &\tau Lb_{1a}\cos\alpha_1\}\end{aligned} \tag{10}$$

The relationship of the distances of these dislocations within coordinate in the formula can be written as

$$\begin{cases}x_{0b}=-l,\ y_{0b}=0,\ x_{0a}=0,\ y_{0a}=0,\\ x_{1ai}=-l-x_i\cos\alpha_1,\ y_{1ai}=x_i\sin\alpha_1\\ x_{1bi}=-x_i\cos\alpha_2,\ y_{1bi}=-x_i\sin\alpha_2\end{cases} \tag{11}$$

where x_i is the distance between the ith GBD and the triple junction; (x_{0b}, y_{0b}) and (x_{0a}, y_{0a}) are the positions of the decomposed dislocations b_{1b} and b_{1a}

in the coordinate. The energy condition that the decomposition transformation of the head dislocation can occur in Fig. 1 is $\Delta E=E_2-E_1<0$.

2.4 Position of blocked dislocations

The position x_i of the blocked GBD can be obtained by solving the first derivative equation of the Laguerre polynomial [37]. The polynomial equation can be expressed as

$$L_i'(x)=-\sum_{k=0}^{i-1}\frac{n!(-x)^k}{k!(k+1)!(n-k-1)!}=0 \tag{12}$$

Taking the case of n=5 as an example, the position of the blocked dislocation x_i can be obtained. If n=5, Eq. (12) becomes

$$L_5'=5-10x+5x^2-\frac{5}{6}x^3+\frac{1}{24}x^4=0 \tag{13}$$

Solving the quadratic equation Eq. (13), four solutions of the equation are obtained: x_2, x_3, x_4 and x_5. The curve of Eq. (13) is shown in Fig. 2. The distance x_i between each dislocation in the pile-up and the triple junction is given in Tables 1 and 2.

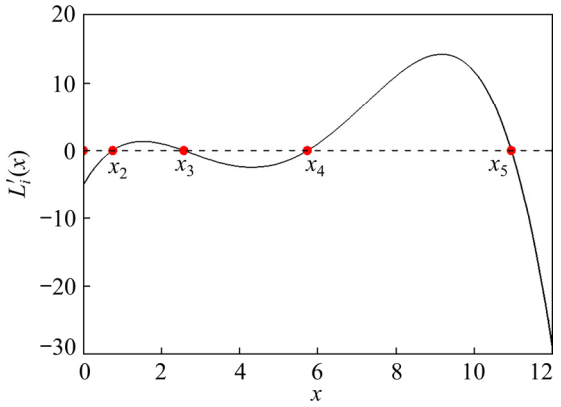

Fig. 2 Curve of L_i' for number n=5 of pile-up of dislocations

Table 1 Distances x_i from pile-up of GBDs to triple junction of grain boundaries when n=5

x_1	x_2	x_3	x_4	x_5
0.0	0.7433	2.5716	5.7312	10.9539

Table 2 Distances x_i from pile-up of GBDs to triple junction of grain boundaries when n=10

x_1	x_2	x_3	x_4	x_5
0.0	0.3682	1.2434	2.6460	4.6169
x_6	x_7	x_8	x_9	x_{10}
7.2218	10.5673	14.8359	20.3822	28.1183

The angles of two Burgers vector of new dislocation b_{1a} and b_{1b} decomposed by the head dislocation at triple junction to the x axis is α_1 and α_2, respectively. For the decomposition of the head dislocation with symmetry $\alpha_1=\alpha_2=\alpha$ and asymmetry $\alpha_1\neq\alpha_2$, their energy barriers of the decomposition of the dislocation with angle α are calculated. It is assumed that the lengths of the pile-up of the dislocation are the same, with the number n=5 and 10 of the blocked GBD at triple junction, respectively. Therefore, the number density of the blocked dislocations at triple junction is higher in the case of n=10, which is 2 times of the case of n=5. According to the above energy model, under the external strains applied to the system, the curves of energy varieties of the system during the dislocation pile-up are calculated by Eq. (10), in which the energy different $\Delta E=E_1-E_2$ depends on the parameters of n, α_1, α_2 and τ. The results are shown in Figs. 3−11, respectively, which are analyzed and discussed as follows.

3 Results and analysis

3.1 Variety of system energy in symmetrical decomposition of head dislocation ($\alpha_1=\alpha_2=\alpha$)

For the pile-up of the GBD at triple junction, the number n=5 of these dislocations is considered. Figure 3 shows the curves of the energy difference ΔE corresponding to the symmetric decomposition of the head dislocation for the number n=5 of the dislocation pile-ups. The abscissa w is the mobile distance L of the dislocation b_{1a}, and the distance from Point A to the origin reflects the thickness L_m of the finite energy barrier in Fig. 3. It can be seen from Fig. 3(a) that the energy variety of the dislocation system for angles α=10°, 20°, 30° and 40° satisfies the energy condition $\Delta E<0$ of the transformation under the stress $\tau=0.0002G$, that is, no energy barrier. At this time, the decomposition of the head dislocation occurs without dislocation pile-up at triple junction. For the energy curves with larger angles α=50°, 60° and 70°, there is $\Delta E>0$ with high energy barrier, which does not satisfy the energy condition of the decomposition transformation. Therefore, in this case, the decomposition of the head dislocation does not occur, and the dislocation is blocked at triple junction. The critical angle α of the structural transformation caused by the blocked head dislocation under the loading of

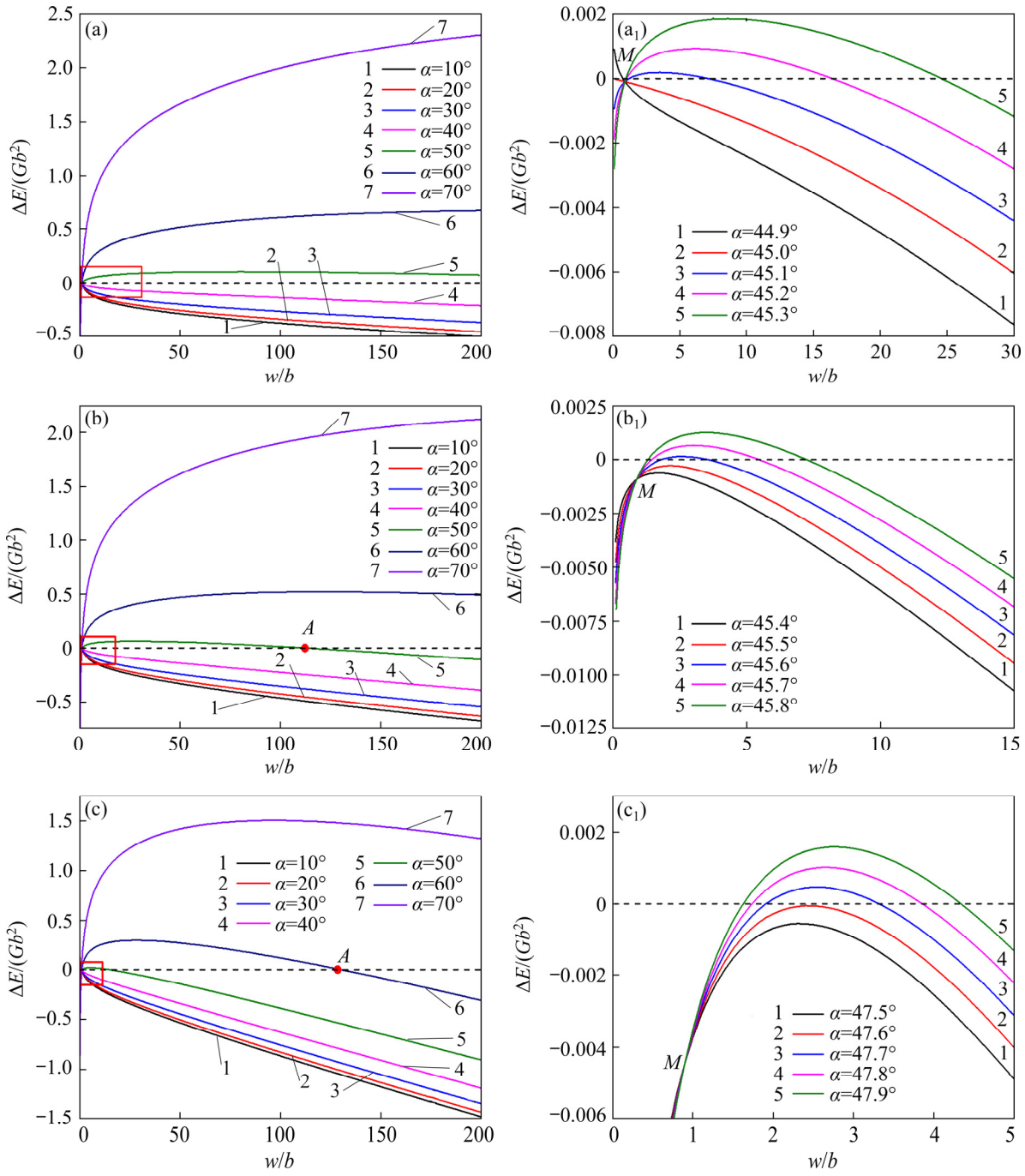

Fig. 3 Curves of energy difference ΔE corresponding to symmetric decomposition of head dislocation for n=5 of dislocation pile-ups: (a, a_1) τ=0.0002G; (b, b_1) τ=0.002G; (c, c_1) τ=0.01G

τ=0.0002G can be obtained from the detailed diagram of energy curves in Fig. 3(a_1), that is α=45.1°. If α>45.1°, there is energy resistance for the head dislocation decomposition. It can be seen from Fig. 3(b) that the stress τ increases to 0.002G, and there is ΔE<0 for the energy curves of α=10°, 20°, 30° and 40°. At this point, there is no energy barrier and no pile-up of the head dislocation, but only the decomposition of the head dislocation occurs. For the curves of α=60° and 70°, the energy barrier is higher to reach $\Delta E \gg 0$, and the energy condition of the decomposition is not satisfied. It can be seen on the energy curve of α=50° in Fig. 3(b), that the dislocation b_{1a} moves and reaches the Point A in which the distance is about 110 atomic units under the external stress. Then, there is a transition because ΔE<0, which results in the decomposition. It can be seen from the curves in

Fig. 3(b_1) that the critical angle of the dislocation structural transition is α=45.6°. With the external stress increasing continuously and reaching τ=0.01G, it can be seen from Fig. 3(c) that, for the dislocation system with α=10°, 20°, 30° and 40°, the energy condition is satisfied with ΔE<0 and the accumulation of the head dislocation does not occur. For the situation with α=70°, the energy condition is not satisfied and the decomposition of the head dislocation does not occur. Nevertheless, for the energy curves of α=50° and 60° in Fig. 3(c), there is a small energy maximum on these energy curves. The dislocation b_{1a} is needed to move a certain distance about 20 atom units for α=50°, under the external stress, while that is about 130 atom units for α=60°, as shown at the Points B and A. At this time, the energy of the system is satisfied with the condition of ΔE<0, which is beneficial to the decomposition of the head dislocation. It can be seen in Fig. 3(c_1) that the critical angle of the decomposition of the blocked head dislocation is about α=47.6°.

By comparing Figs. 3(a−c), it can be seen that it is beneficial to the decomposition of the head dislocation in small angle, while it is difficult to realize for the decomposition of the dislocation in large angle. There is a critical angle for the transition between two decomposition dislocations. With the increase of the external stress τ, the critical angle $\alpha_1+\alpha_2=2\alpha$ of the head dislocation decomposition is in the range from 90° to 95.2°. It is indicated that an applied external force τ is conducive to increase the critical angle of the head dislocation decomposition.

The energy curves of the dislocation pile-up in the system are shown in Figs. 4(a−c) for the case of the GBD pile-up at triple junction with n=10. It can be seen from Fig. 4(a) under τ=0.0002G, that energy curves for α=10°, 20°, 30° and 40° are negative, i.e. ΔE<0; while the energy curves for α= 60° and 70° are positive. Because of the large energy barrier for the larger angle, the blocked head dislocation does not undergo decomposition. However, for the energy curve of α=50°, there is only tiny energy maximum. In this case, the condition of ΔE<0 is satisfied under the external stress, as shown in Fig. 4(a). At this time, the transition of the dislocation structure occurs, and the corresponding critical angle given in Fig. 4(a1) is α=45.1°. In Fig. 4(b), it can be seen that the energy curves of α=10°, 20°, 30° and 40° remain negative when the applied external force reaches τ=0.002G, i.e., it is satisfied with ΔE<0. This indicates that the decomposition of the head dislocation can occur. For the energy curves of α=60° and 70°, there is a energy barrier on each curve, and thus the decomposition transition of the blocked head dislocation cannot occur. However, for the energy curve of α=50°, it can be seen in Fig. 4(b) that there is only one tiny energy barrier. The curve is intersected by x axis of ΔE=0 at the Point A, which indicates that the decomposition transformation of the head dislocation can be realized under the external stress. The critical angle of the head dislocation transformation allowed by the energy condition is α=45.1°. In Fig. 4(c), it can be seen that when the applied external force reaches τ=0.01G, the energy curves of α=10°, 20°, 30° and 40° satisfy ΔE<0, and the head dislocation can be decomposed. For the energy curves of α=70° with a large energy barrier, the head dislocation is not decomposed. While for energy curves of α=50° and 60°, the energy of the system becomes negative at Point A on the energy curve of α=60° and Point B on the energy curve of α=50° under larger external stress. The critical angle α=47.5° of the structural transition of the head dislocation is shown on the energy curve of Fig. 4(c1).

By comparing the results of Figs. 4(a−c), it can be seen that the head dislocation decomposition with the smaller angle is easier to proceed. The larger the angle of the head dislocation decomposition is, the greater the energy barrier is, and the harder the decomposition transformation is. With the increase of external stress τ, the critical angle $2\alpha=\alpha_1+\alpha_2$ of the head dislocation decomposition increases from 90° to 95.0°, and the height of energy curve decreases with the increase of external stress τ. This indicates that the increase of external stress τ is beneficial to the decomposition transition of the head dislocation.

3.2 System energy of decomposition transition with asymmetric angle ($\alpha_1\neq\alpha_2$)

3.2.1 α_1=30° with α_2 changed

(1) When the external stress is small at τ=0.0002G, ΔE<0 is satisfied for the energy curve of α_2=40° or 50° with n=5, as shown in Fig. 5(a). Therefore, the decomposition transformation of the head dislocation occurs. For energy curves of

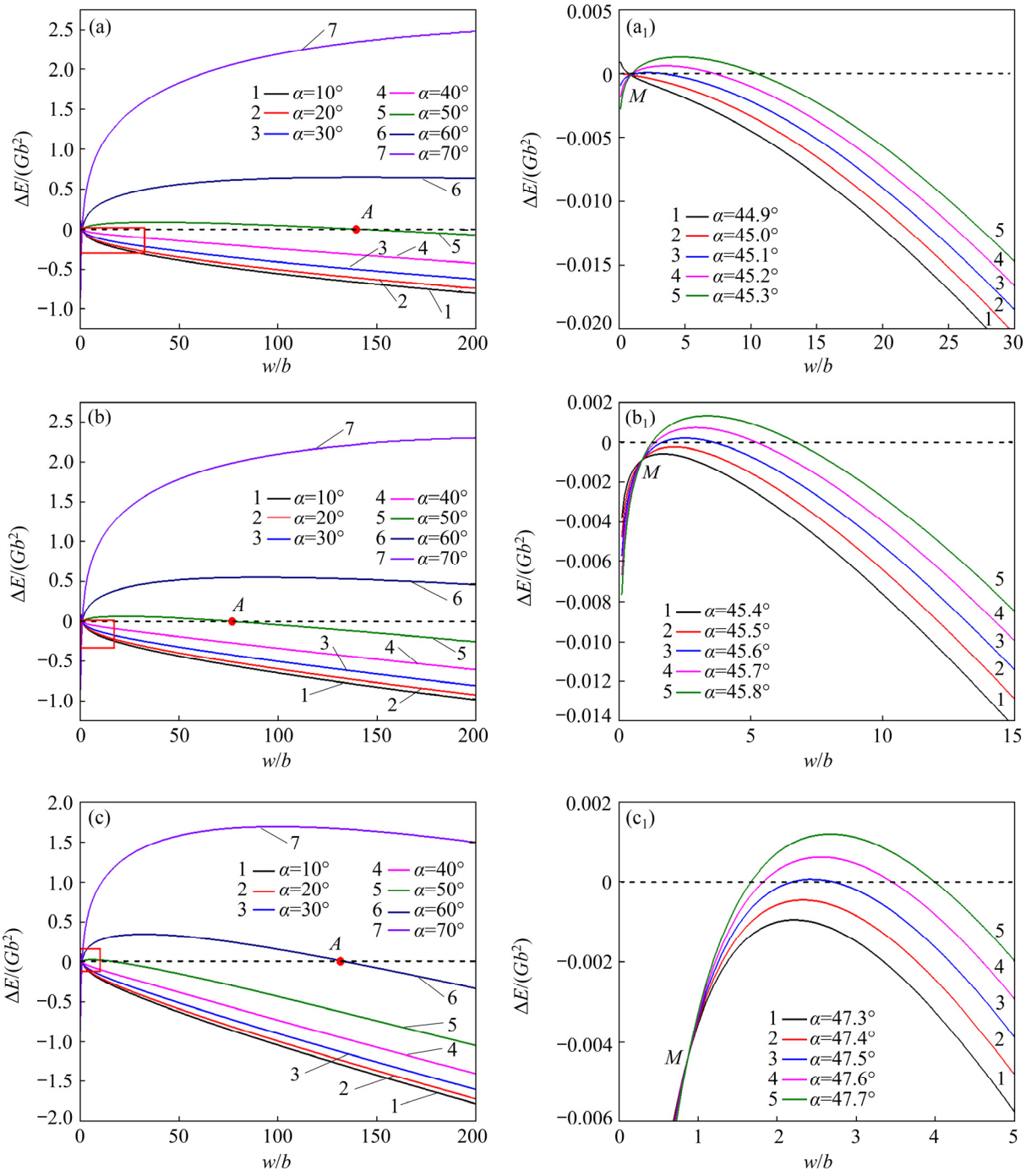

Fig. 4 Curves of energy difference ΔE corresponding to symmetric decomposition of head dislocation for n=10 of dislocation pile-ups: (a, a_1) τ=0.0002G; (b, b_1) τ=0.002G; (c, c_1) τ=0.01G

α_2=70° and 80°, because of large energy barrier, the decomposition transition of the head dislocation does not occur. For the case of α_2=60°, under the external stress, the energy barrier of the decomposition transition can be eliminated. It can be seen from Fig. 5(a_1) that the critical angle of the transformation of the head dislocation is α_2=57.9°. When τ=0.002G, it can be seen from Fig. 5(b) that the energy curves of α_2=40°, 50° and 60° are satisfied with the condition of the head dislocation decomposition. In Fig. 5(b_1), the energy curve of α_2=60° is just the critical energy curve with energy barrier equal to zero, while for the energy curves of α_2=70° and 80°, because of $\Delta E \gg 0$, the head dislocation cannot be decomposed. When τ=0.01G and α_2=40°, 50° and 60°, the reaction of

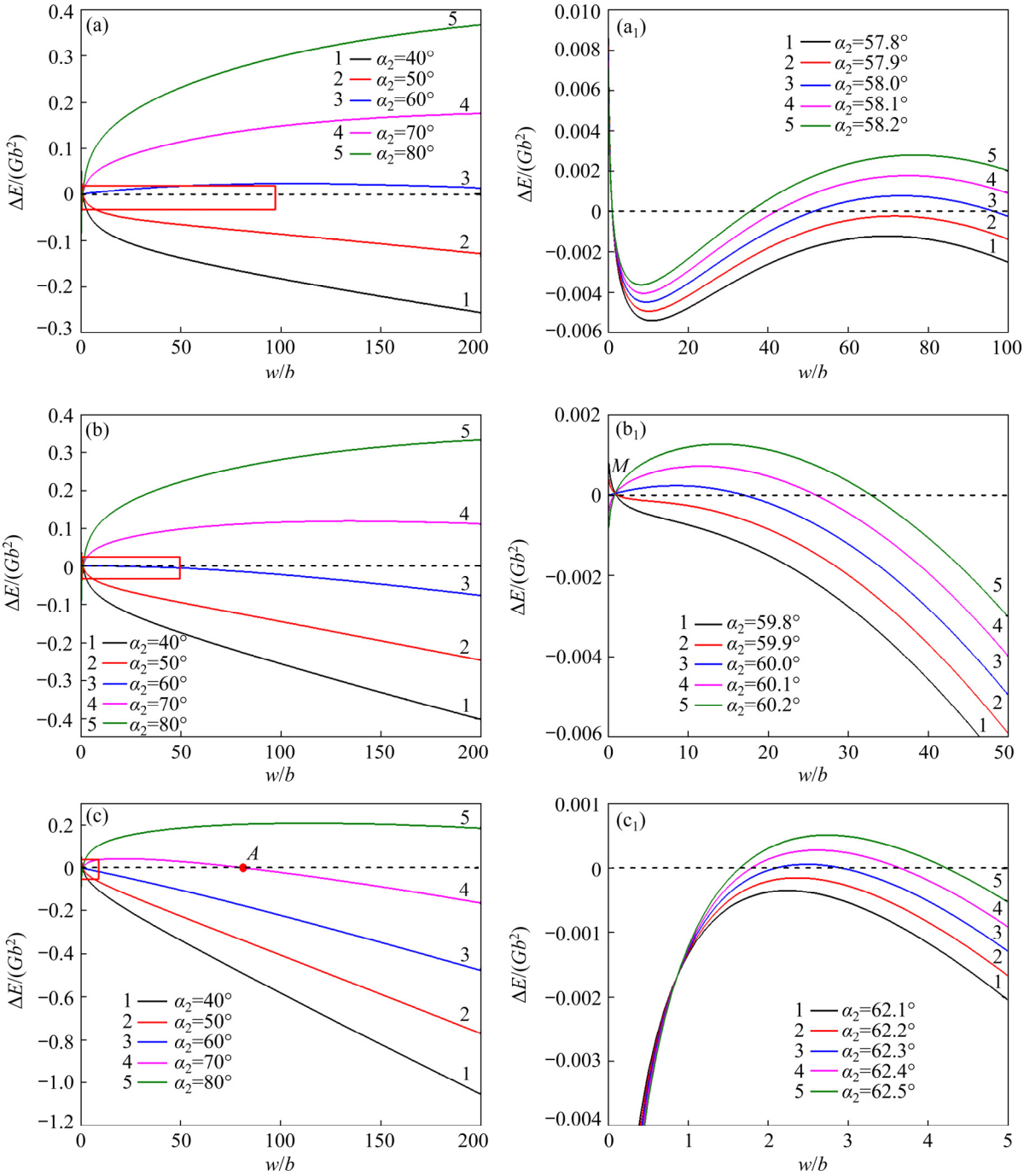

Fig. 5 Curves of energy difference ΔE corresponding to asymmetric decomposition of head dislocation for n=5 and α_1=30° of dislocation pile-ups with α_2 taking different values: (a, a$_1$) τ=0.0002G; (b, b$_1$) τ=0.002G; (c, c$_1$) τ=0.01G

decomposition of the head dislocation can occur, as shown in Fig. 5(c). However, for α=70°, there is a smaller energy barrier. Therefore, the decomposition of the head dislocation can be carried on when ΔE<0 is satisfied under the external stress. For α_2=80°, the head dislocation cannot be decomposed with $\Delta E \gg 0$. The critical angle of the transition is α_2=62.3° under the condition of τ=0.01G.

(2) There are some details in the case of n=10, which are similar to the case of n=5. It can be seen in Fig. 6(a), when τ=0.0002G, the decomposition of the head dislocation can occur with the smaller angles α_2=40° and 50°, while it cannot occur with larger angles α=70° and 80°. It can be seen in the energy curve of α_2=60° in Fig. 6(a) that there is a finite energy barrier. Under the stress, the energy barrier disappears and the decomposition of the

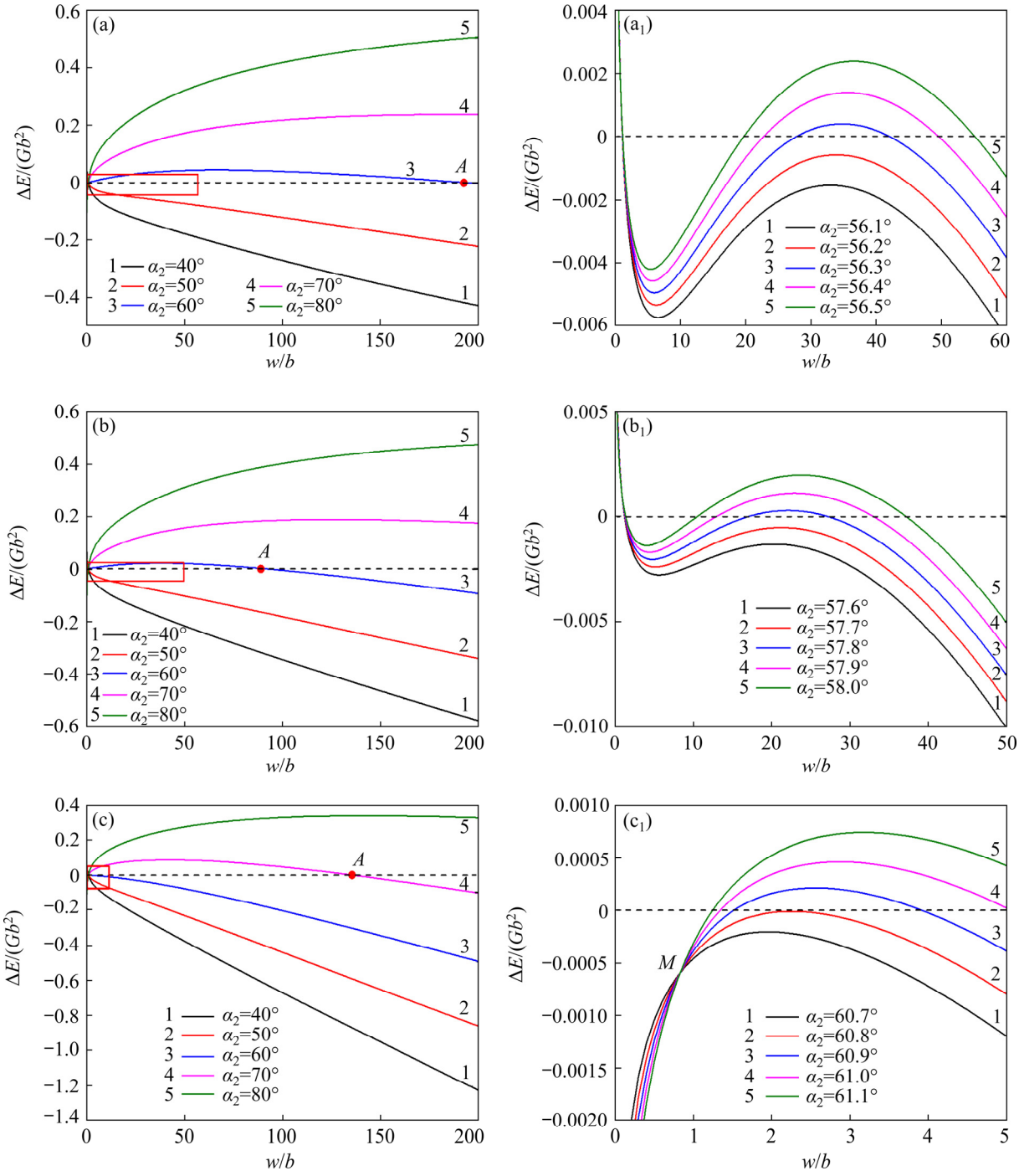

Fig. 6 Curves of energy difference ΔE corresponding to asymmetric decomposition of head dislocation for n=10 and α_1=30° of dislocation pile-ups with α_2 taking different values: (a, a_1) r=0.0002G; (b, b_1) r=0.002G; (c, c_1) r=0.01G

head dislocation can be carried out smoothly. As shown in Fig. 6(a_1), the critical angle of the dislocation transition is α_2=56.2°. With τ=0.002G and α_2=40° or 50°, as shown in Fig. 6(b), the decomposition of the head dislocation can occur. Owing to the large barrier on the curves of α=70° and 80°, the decomposition of the head dislocation cannot occur. For the energy curve of α_2=60°, under the external stress, the barrier disappears, as shown at Point A in Fig. 6(b). At this time, the decomposition of the head dislocation occurs with the critical angle α_2=57.7°. Under the stress τ=0.01G, the rule shown in Fig. 6(c) is similar to that in Fig. 6(b). At this time, the energy on curves of α_2=40° and 50° is negative, and the energy on curve of α_2=60° changes from positive to negative,

while for that of α_2=70°, there is a small energy maximum in the energy curve. It can be seen from Fig. 6(c) that the barrier disappears with ΔE<0, and under the external stress, and the decomposition transformation can be realized. The critical angle of the head dislocation transition increases to 60.8°.

By comparing Figs. 6(a−c), it can be seen that the critical angle α_2 of the head dislocation decomposition increases from 56.2° to 60.8° with increasing τ, and at the same time, the vector angle between two new decomposed dislocations increases from $\alpha_1+\alpha_2$=86.2 to 90.8°. The increasing value of the external stress τ is beneficial to the decomposition of the head dislocation.

3.2.2 α_2=50° with α_1 changed

(1) For the case of n=5, as shown in Fig. 7(a), under the external stress τ=0.0002G, the energy on curves of α_1=20° and 30° are satisfied with the condition of ΔE<0, and therefore the decomposition of the head dislocation can occur; while for α_1=50°

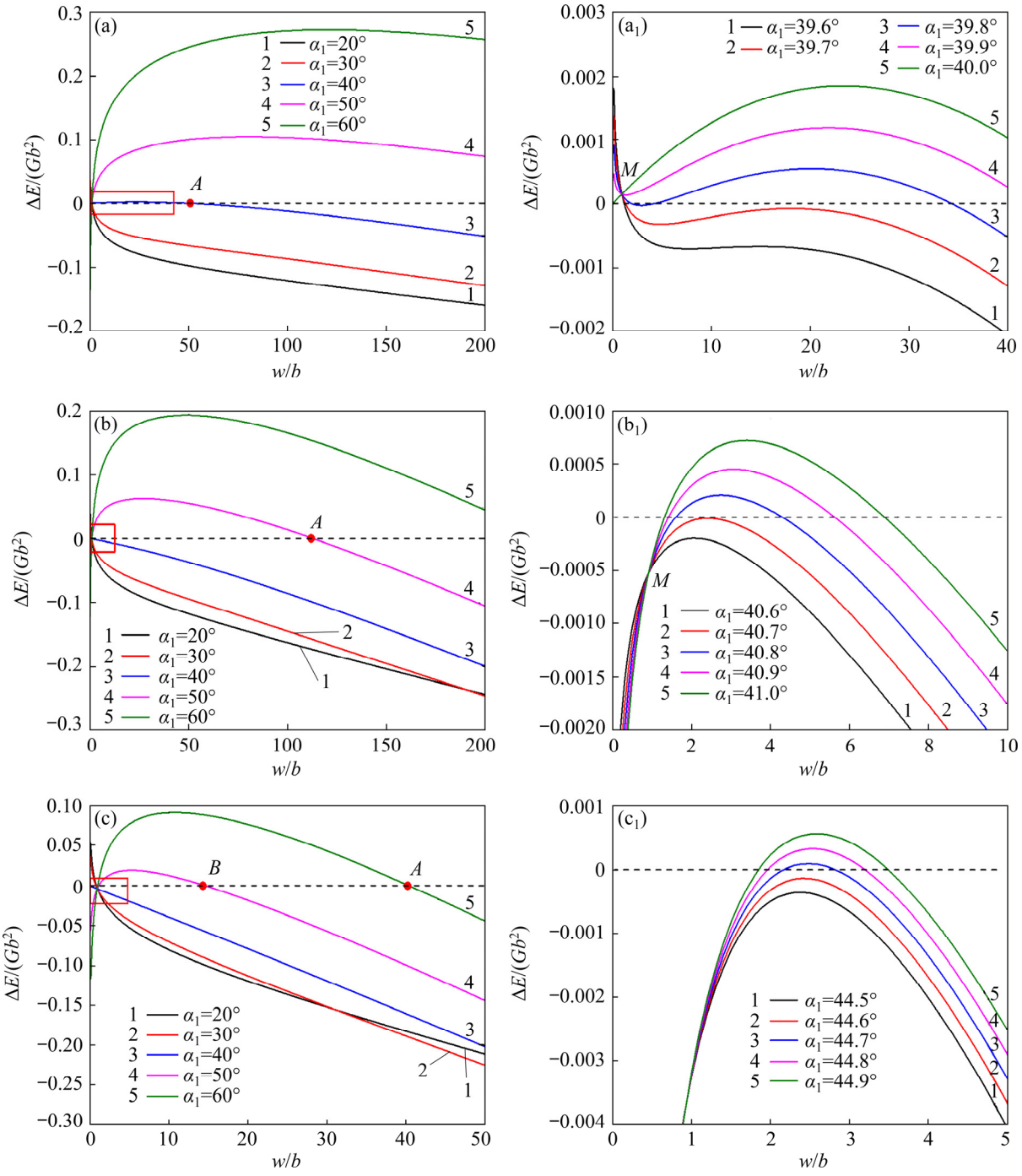

Fig. 7 Curves of energy difference ΔE corresponding to asymmetric orientation decomposition of head dislocation for α_2=50° of dislocation pile-ups with α_1 taking different values: (a, a$_1$) r=0.0002G; (b, b$_1$) r=0.002G; (c, c$_1$) r=0.01G

and 60°, there is a large barrier in the energy of the system, that is $\Delta E \gg 0$, so the head dislocation is difficult to decompose. For α_1=40°, there is only a small barrier on the energy curve, and at this time, the decomposition of the head dislocation can be realized under the external stress τ. As shown in the Fig. 7(a_1), the critical angle of the decomposition is α_1=36.7°. When the applied stress reaches τ=0.002G, it can be seen from Fig. 7(b) that the energy on curves of α_1=20°, 30° and 40° are negative, and the decomposition of the head dislocation occurs. In Fig. 7(b_1), for the larger angle α_1=50°, there is a transition in which the energy value changes from positive to negative on the energy curve, so the decomposition of the head dislocation can be realized under the stress τ. For the energy curve with α=60°, the decomposition transformation does not occur due to $\Delta E \gg 0$. The critical angle of the decomposition is α_2=40.7° at τ=0.002G. When the applied stress reaches τ=0.01G, as shown in Fig. 7(c), in the situation similar to Fig. 7(b), the energy curves of α_1=20°, 30° and 40° are completely negative. However, for the energy curves of α=50° and 60°, the energy changes from positive to negative under the external stress. At this time, ΔE<0 is satisfied, and therefore, the decomposition transformation of the head dislocation can be carried out. The critical angle of the dislocation transition is α_1=44.7° for the stress τ=0.01G. By comparing Figs. 7(a−c), it can be seen that the head dislocation decomposition with smaller angle is easier to proceed. With the increase of τ, the critical angle increases from $\alpha_1+\alpha_2$=86.7° to 94.7°. The value of external stress τ increasing is beneficial to the decomposition transformation of the head dislocation.

(2) For the case of n=10, the results are similar to the curves in Fig. 7, while there are some differences in details. As shown in Fig. 8(a), in the condition of τ=0.0002G, for α_1=20° and 30°, the decomposition of the head dislocation can be realized, while for α=60°, the decomposition of the head dislocation does not occur. For the energy curves of α_1=40° and 50° in Fig. 8(a), there is a finite energy maximum, and the corresponding barrier disappears at Point A with ΔE<0. This indicates that the decomposition transition of the head dislocation can proceed smoothly under the external stress at the angle α_1=40° and 50°. Under the action of τ=0.0002G, the critical angle of the dislocation decomposition is α_1=39.0°. As shown in Fig. 8(b), under the external stress τ=0.002G, three energy curves of α_1=20°, 30° and 40° are negative, and therefore the decomposition transformation of the head dislocation can be realized. It is similar to the case in Fig. 7(c) that energy curves of α_1=50° and 60° are obviously reduced, and the energy value converts to zero under the stress τ=0.002G. At the same time, the system satisfies ΔE<0 and the decomposition transformation of the head dislocation can be realized. Under the stress τ=0.002G, the critical angle of the dislocation decomposition is α_2=40°. The change law of the energy curves is similar to that in Fig. 8(b) under τ=0.01G. At this time, three energy curves of α_1=20°, 30° and 40° are negative, which causes the decomposition transition of the head dislocation to be realized. By comparing with Fig. 8(b), it can be seen that the heights of the energy curves for α_1=50° and 60° are obviously reduced, and therefore the condition of ΔE<0 can be realized under the action of τ=0.01G, and the head dislocation can be decomposed. Under the stress τ=0.01G, the critical transition angle of the head dislocation is α_2=44.8°.

Figures 8(a−c) show that the critical transition angle α_1 of the head dislocation increases from 39.0° to 44.0° with the increasing of τ. At the same time, the critical angle $\alpha_1+\alpha_2$=89.0° increases to 94.8°. Therefore, the increase of external stress τ is beneficial to the decomposition of the head dislocation, which makes the state of the energy curve transform from high energy barrier to the low one, and even transform from a finite energy barrier to absence.

3.3 Height of energy extreme and thickness of energy barrier

The variation curve of the energy height ΔE_m of the head dislocation decomposition along with external stress τ changing for n=5 and n=10 are given in Figs. 9(a, b), respectively. It can be seen from Fig. 9(a) that ΔE_m of the energy extreme is the highest for the energy curve with $\alpha_1+\alpha_2$=46°+50°, while the lowest for the curve with $\alpha_1+\alpha_2$=50°+46°, and the middle for $\alpha_1+\alpha_2$=48°+48°. The peak value decreases with the increase of the external stress τ, in which the transformation law of these curves is the same. All these results show that the external stress τ is beneficial to the energy transition from

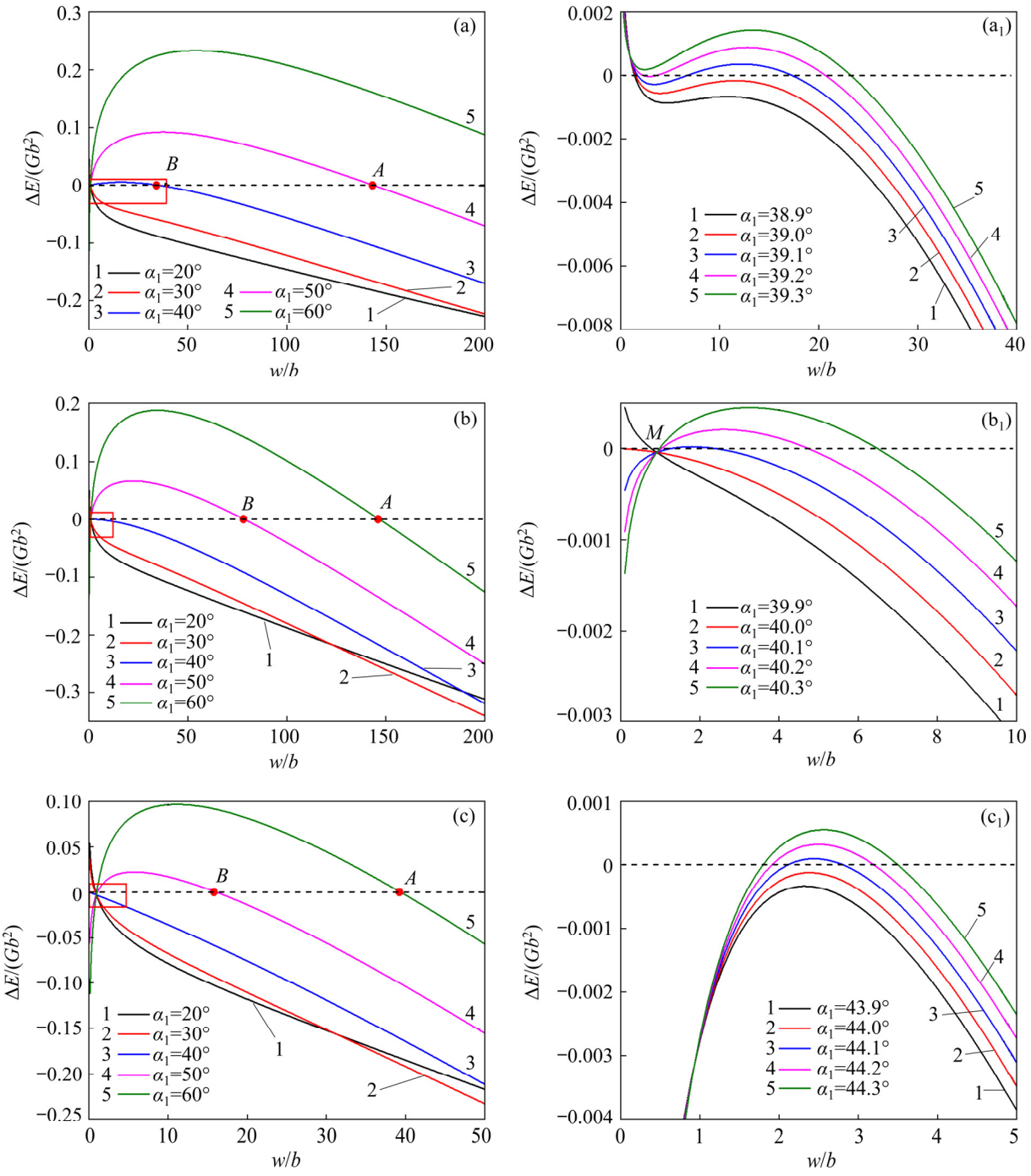

Fig. 8 Curves of energy difference ΔE corresponding to asymmetric orientation decomposition of head dislocation for n=10 and α_2=50° of dislocation pile-ups with α_1 taking different values: (a, a_1) r=0.0002G; (b, b_1) r=0.002G; (c, c_1) r=0.01G

positive to negative. It can be found that when the angle $\alpha_1+\alpha_2$=96° is fixed, the smaller the orientation angle α_1 of the mobile dislocation b_{ia} is, the lower the value of the energy extreme, and the larger the α_1 is, the higher the value of the energy extreme. As a result, under such conditions, the transformation of the dislocation decomposition will occur with lower orientation angle α_1 as far as possible. In Fig. 9(b), it can be seen that the case of n=10 is generally similar to that of n=5. Comparing the cases n=5 and n=10 in Figs. 9(a, b), we can also see the height of the energy extreme value ΔE_m corresponds to the cases with three kinds of angle configurations. When the external stress is

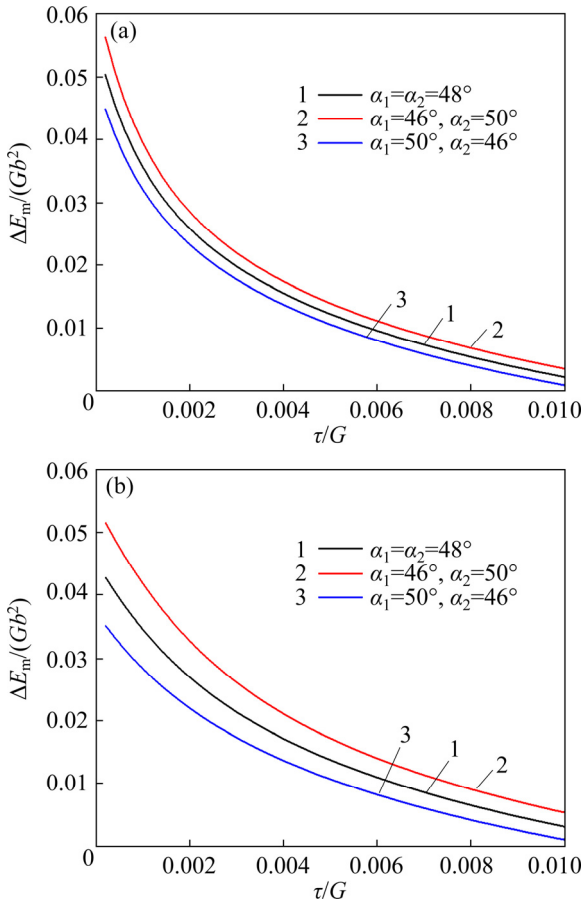

Fig. 9 Curves of energy barrier height for symmetric decomposition of head dislocation and asymmetric decomposition under external stress: (a) n=5; (b) n=10

relatively small, the energy barrier ΔE_m of n=10 is lower, and the relative difference of the height of the energy barrier is larger. This shows that the increase of n has a great influence on the height of the energy extreme with different angle configurations. The height of the energy barrier tends to be consistent for n=5 and 10 under the action of large stress.

Figure 10(a) shows that the thickness L of the energy barrier for the dislocation decomposition with three different orientation angles decreases with the external stress τ increasing. Therefore, it can be seen that when there is no external stress τ or the external stress τ is very low, and the thickness L of the energy barrier for n=10 is smaller than that for n=5. From the view of angle orientation configuration, the lower the α_1 is, the smaller the thickness of the energy barrier is, and the larger the angle α_1 is, the larger the thickness is. When the external stress τ is large, the influence of n is weakened, and the curves of n=5 and 10 tend to be consistent, as shown in Fig. 10(a). It can be seen that the decomposition transformation of the head dislocation is promoted by the external stress. Figure 11 shows the nonlinear monotone curves of the barrier thickness L_m corresponding to the decomposition transition of the head dislocation with the number n of the dislocation piled-ups

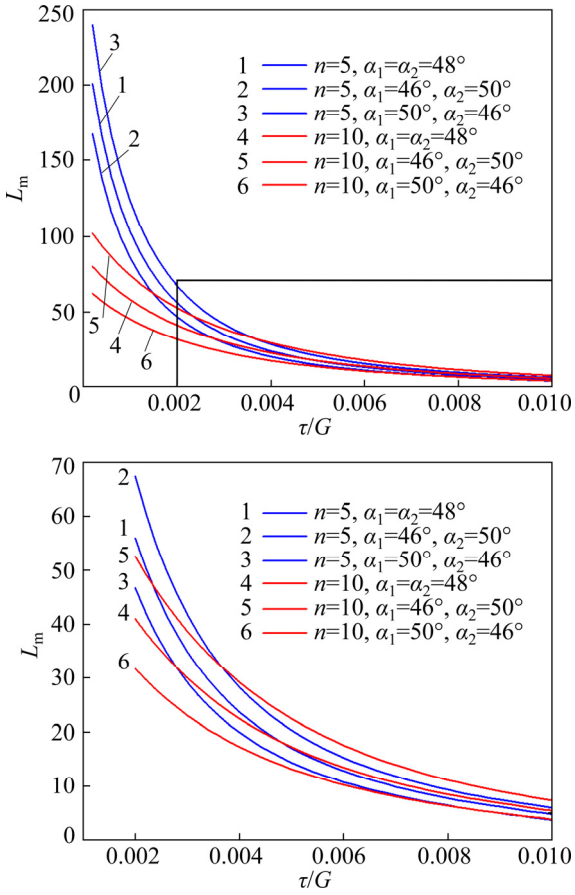

Fig. 10 Characteristic curves of peak position of energy barrier changing with external stress

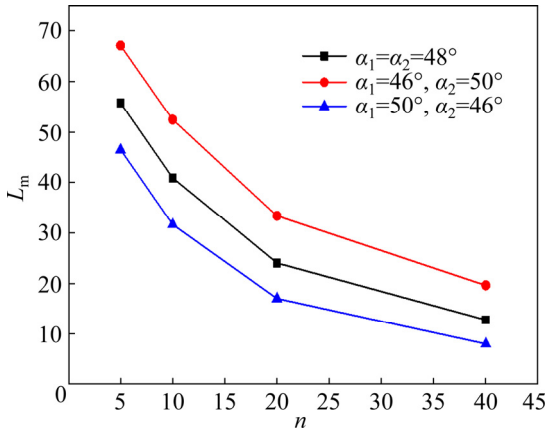

Fig. 11 Curves of energy barrier thickness L_m of decomposition transformation of head dislocation with n of dislocation pile-up under external stress τ=0.002G

increasing under the external stress τ=0.002G. It can be seen from Fig. 11 that the larger the n is, the smaller the value of distance L_m is. For example, in the decomposition transition of the dislocation with α_1=α_2=48°, the barrier thickness L_m=55 corresponds to the case of n=5, and L_m=40 for n=10, L_m=25 for n=20, and L_m=13 for n=40. As a result, the larger number n of the dislocation piled-ups is more favorable for the head dislocation to overcome the resistance of energy barrier and realize decomposition transition.

3.4 Discussion

According to the above calculation results, it can be seen that the head dislocation of the GBD pile-up can be decomposed at the triple junction in a wide range of the angle orientation parameter, because the GBD can be accumulated as a container of strain concentration at the triple junction. In this case, the stress concentration can be released by the decomposition transition, which inhibits the crack initiation and fracture. Therefore, the GB moving as plastic deformation channel is strongly affected by the geometric characteristic of the head dislocation decomposition of the GBD pile-up. The decomposition of the GBD at triple junction can be carried out effectively if the orientation angle α_1 and α_2 of the decomposition are small enough. In such case, under the external stress, the triple junction points can be naturally distinguished into so-called “hardened” and “softened” ones. By using the model principle of the GBD decomposition at triple junction, the hardening and softening phenomena in ultrafine-grained materials and the mutual transformation between hardening and softening in nanocrystalline materials can be analyzed and discussed. For example, if there is no decomposition transition when the GBD are accumulated at triple junction, such triple junction is called a hard triple junction. Conversely, if the decomposition transition occurs and is accompanied by new mobile dislocations moving along the adjacent grain boundary, such triple junction is called a soft triple junction. Now, we regard the number of the hard triple junction in ultrafine-grained or nanocrystalline materials as N_h and the number of the soft triple junction as N_s. The conventional deformation mechanism is changed from individual dislocation moving to collective moving of the GB (dislocation), which can be considered as the transformation of deformation mechanism in nanocrystalline materials. On the basis of the model principle of this work, the key role of the competition between the deformation mechanism of the GBD moving and other mechanisms in nanocrystalline materials can be explained by ratio N_s/N_h, the high value of which indicates strong characteristic of the GB moving, i.e. the value of yield stress is lower than that of the other deformation mechanism. If plastic flow appears with low N_s/N_h in the materials, it may be the result of another deformation mechanism, because the conventional slipping of the grain boundary is inhibited.

In this work, the modes of the decomposition transition of the blocked GBD at triple junction and of the mobile dislocation along grain boundary are considered. Based on this decomposition mode, the property of strong ductility in ultrafine-grained metal materials can be effectively explained, as well as the transformation of strengthening and softening in ultrafine-grained metal materials, even the phenomenon of superplastic deformation. The influence on deformation behavior and the motion of the GB by the decomposition transformation of the blocked GBD at triple junction are contributed to the transition of triple junction from hard to soft. It can be explained that the observed plastic flow is localized because the migration of the GB induces the transformation of the triple junction to become soft due to the local movement of the GB in these regions, and thus the localization of the plastic flow is enhanced. According to the decomposition of the blocked dislocation at the triple junction, the formation of the immobile dislocation plays a strengthening and hardening role, while the mobile dislocation can release strain energy, which plays the soften role and improves the plasticity. In this case, crack initiation is inhibited and plasticity is improved.

We note that the GBD pile-up can continuously undergo the dislocation decomposition at the triple junction and produce immobile dislocation, which can cause the immobile dislocation generated at the triple junction to form a large immobile dislocation by merging through controlling the orientation angle of the decomposition. By expanding the model based on this idea, we can establish a large dislocation model and apply it to nanocrack initiation, and reveal the

nucleation and initiation mechanism of nano-crack [41−43] at the triple junction. We can also apply the model to the accumulation and merging of the immobile dislocation generated at the triple junction to form large multiple Burgers vector of the immobile dislocation and to result in the strengthening effect of nanocrystalline materials. We can use the external stress to control the angle of Burgers vector of the decomposition dislocation [44], so that the barrier of the dislocation decomposition is reduced, and the mechanism of softening and superplastic deformation is revealed. The calculation results of the model in this work are supported and confirmed by the results of the experiments [45] and other simulation method [46].

The traditional dislocation pile-up model [6] is mainly a sequence of dislocations generated by a dislocation source, which stops moving when encountering obstacles during the movement processes, and these dislocations have a pile-up arrangement. The head dislocation of the piled-up GBD generates stress concentration. If the head dislocation is blocked by a second phase particle, a crack nucleation may be induced near the second phase particles when the stress of the dislocation of the piled-up GBD reaches a critical value. The dislocation pile-up energy model at the triple junctions of grain boundaries in this work describes that the piled-up GBD of dislocations at the triple junctions has a grain boundary strengthening effect; On the other hand, when the stress concentration of the head dislocation of the piled-up GBD reaches a critical value, the decomposition reaction of the head dislocation occurs. The dislocation decomposition causes the dislocation moving from the triple junctions to release the strain energy and the grain boundaries are softened, which is beneficial to the sliding deformation and improving the plasticity of the material. This is the largest difference from the model for traditional dislocation pile-up.

There are same reports [47−49] about the decomposition of dislocations pile-up at grain boundaries and triple junctions of grain boundaries in the references. Under the guidance of such experimental results, the model established in this work conforms to the favorable conditions of energy change. There are two kinds of dislocations in grain boundary: one is an immobile dislocation and the other is a movable dislocation [49]. One of the dislocations decomposed is an immobile dislocation and the other is movable, which is physically reasonable because it conforms to the reduction law of the energy change. The dislocation decomposition and slip reflect the softening of the grain boundaries, which is related to the reverse Hall−Petch effect [4]. At this time, the dislocation sliding along the grain boundary is different from the intragranular slip, and it is more of the zig-zag propagation between the grain boundary atoms [50].

The limitations of the energy model in the application is that when the grain size is less than 10 nm, the dislocation decomposition reaction may have a new change in the case of the dislocation pile-up in this model. For example, the two new dislocations in the head dislocation decomposition may each move along the two grain boundaries, and the grain boundary becomes soft and the strengthening effect is weakened. This situation has been experimentally confirmed [47]. Indeed, the dislocation transmission across the GB is a tricky and complicated issue. In this work, a simplified physical model is proposed to describe the decomposition of the dislocation pile-up at the triple junctions of the grain boundaries. The results obtained by the model can well explain the basic characteristics of the strengthening, toughening and softening of ultrafine grains and nanocrystalline materials. However, the detailed description of the dislocation transmission on the grain boundary by the model is not detailed enough. Dealing with the tricky problem, molecular dynamics simulations are needed to give the specific details of the dislocation transmission.

The physical energy model in this work is the two-dimensional model in the (x, y) plane. This model describes the movement and interaction of dislocations in the plane, in which the path of the dislocation movement is a straight line. In the model, only the dislocation pile-up of a triple junction of the grain boundary and the dislocation decomposition are considered. The situation actually exists. Although the decomposition motion of the dislocation considered in this model is in a line, it can describe the movement of the dislocation in a short distance. The cross slipping in real situation may occur, but it is more complicated, which is not considered in this model. For the case

of the decomposition appearing at all triple junctions around the three grains, we believe that this situation may occur, but the possibility of simultaneous occurrence will be very small. Therefore, the dislocation of a certain triple junction to start decomposition in this work is only considered at first, while for other dislocations in the triple junction of the surrounding grains the conditions for starting decomposition does not meet.

4 Conclusions

(1) A phenomenological energy model for the decomposition of the GBD is proposed to calculate the systematic energy variation of the structure transformation of the GBD under an external stress. When the GBD is accumulated at triple junction, the head dislocation of the GBD can be decomposed into two new dislocations unless the angle between the two Burgers vectors of these dislocations is less than 90°.

(2) The more the number of the pile-up of the GBD at triple junction of the GB is, the more favorable the decomposition of the head dislocation is. The increase of applied external stress can reduce the energy resistance of the dislocation decomposition to make the high energy barrier change to the low one, and even to make the barrier with finite height disappear and promote the decomposition transition of the GBD.

(3) The energy model of the decomposition of the GBD at triple junction can well exhibit the variation characteristics of the system energy during the GBD decomposition under the action of external stress, and well reveal that the energy conditions of the decomposition of the GBD at triple junction can be regulated by the action of external stress.

Acknowledgments

The authors are grateful for the financial supports from the National Natural Science Foundation of China (Nos. 51161003, 51561031), and the Natural Science Foundation of Guangxi, China (No. 2018GXNSFAA138150).

References

[1] TRIMBY P W, CAO Y, CHEN Z, HAN S, HEMKER K J, LIAN J, LIAO X, ROTTMANN P, SAMUDRALA S, SUN J, WANG J T, WHEELER J, CAIRNEY J M. Characterizing deformed ultrafine-grained and nanocrystalline materials using transmission Kikuchi diffraction in a scanning electron microscope [J]. Acta Materialia, 2014, 62: 69−80.

[2] DOLLÁR M, DOLLÁR A. On the strength and ductility of nanocrystalline materials [J]. Journal of Materials Processing Technology, 2004, 157/158: 491−495.

[3] AMES I M, GREWER M, BRAUN C, BIRRINGER R. Nanocrystalline metals go ductile under shear deformation [J]. Materials Science and Engineering A, 2012, 546: 248−256.

[4] CARLTON C E, FERREIRA P J. What is behind the inverse Hall–Petch effect in nanocrystalline materials? [J]. Acta Materialia, 2007, 55: 3749−3756.

[5] HALL C L. Asymptotic analysis of a pile-up of regular edge dislocation walls [J]. Materials Science and Engineering A, 2011, 530: 144−148.

[6] HIRTH J P, LOTHE J. Theory of dislocations [M]. 2nd ed. New York: Wiley, 1968.

[7] LIU C H, LU W J, WENG G J, LI J J. A cooperative nano-grain rotation and grain-boundary migration mechanism for enhanced dislocation emission and tensile ductility in nanocrystalline materials [J]. Materials Science and Engineering A, 2019, 756: 284−290.

[8] MORRIS S J S, JACKSON I. Diffusionally assisted grain-boundary sliding and viscoelasticity of polycrystals [J]. Journal of the Mechanics and Physics of Solids, 2009, 57: 744−761.

[9] GUTKIN M Y, OVID'KO I A, SKIBA N V. Crossover from grain boundary sliding to rotational deformation in nanocrystalline materials [J]. Acta Materialia, 2003, 51: 4059−4071.

[10] LEVITAS V I. Strain-induced nucleation at a dislocation pile-up: A nanoscale model for high pressure mechanochemistry [J]. Physics Letters A, 2004, 327: 180−185.

[11] TANG Xiao-zhi, ZHANG Hui-shi, GUO Ya-fang. Atomistic simulations of interactions between screw dislocation and twin boundaries in zirconium [J]. Transactions of Nonferrous Metals Society of China, 2018, 28: 1192−1199.

[12] OVID'KO I A, SHEINERMAN A G. Free surface effects on stress-driven grain boundary sliding and migration processes in nanocrystalline materials [J]. Acta Materialia, 2016, 121: 117−125.

[13] OVID'KO I A, SHEINERMAN A G. Generation of cracks at triple junctions of grain boundaries in mechanically loaded polysilicon [J]. Philosophical Magazine, 2007, 87: 4181−4195.

[14] LI X T, JIANG X Y. Effects of dislocation pile-up and nanocracks on the main crack propagation in crystalline metals under uniaxial tensile load [J]. Engineering Fracture Mechanics, 2019, 212: 258−268.

[15] ZHAO Y X, XU L Y. Effect of blunt nanocracks on the splitting transformation of grain boundary dislocation piled up at triple junctions [J]. International Journal of Solids and Structures, 2018, 141/142: 232−244.

[16] ZHANG Y Q, JIANG S Y, ZHU X M, SUN D. Orientation dependence of void growth at triple junction of grain

boundaries in nanoscale tricrystal nickel film subjected to uniaxial tensile loading [J]. Journal of Physics and Chemistry of Solids, 2016, 98: 220−232.

[17] ZHANG X H. A continuum model for dislocation pile-up problems [J]. Acta Materialia, 2017, 128: 428−439.

[18] KOBAYASHI S, TSUREKAWA S, WATANABE T. Roles of structure-dependent hardening at grain boundaries and triple junctions in deformation and fracture of molybdenum polycrystals [J]. Materials Science and Engineering A, 2008, 483−484: 712−715.

[19] TIAN Xiao-lin, ZHAO Yu-hong, PENG Dun-wei, GUO Qing-wei, GUO Zhen, HOU Hua. Phase-field crystal simulation of evolution of liquid pools in grain boundary pre-melting regions [J]. Transactions of Nonferrous Metals Society of China, 2021, 31: 1175−1188.

[20] SHI Zhang-zhi, WANG Hai-peng, LIU Xue-feng. Significant influence of sharp grain boundary corner on tensile elongation of copper bars with columnar grains and its mechanism [J]. Transactions of Nonferrous Metals Society of China, 2018, 28: 1329−1333.

[21] MALOPHEYEV S, VYSOTSKIY I, MIRONOV S, KAIBYSHEV R. Is Ashby grain-boundary hardening model applicable for high strains? [J]. Transactions of Nonferrous Metals Society of China, 2019, 29: 2245−2251.

[22] KOBAYASHI S, TSUREKAWA S, WATANABE T. Grain boundary hardening and triple junction hardening in polycrystalline molybdenum [J]. Acta Materialia, 2005, 53: 1051−1057.

[23] EISENHUT L, SCHAEFER F, GRUENEWALD P, WEITER L, MARX M, MOTZ C. Effect of a dislocation pile-up at the neutral axis on trans-crystalline crack growth for micro-bending fatigue [J]. International Journal of Fatigue, 2017, 94: 131−139.

[24] OVID'KO I A, SHEINERMAN A G. Suppression of nanocrack generation in nanocrystalline materials under superplastic deformation [J]. Acta Materialia, 2005, 53: 1347−1359.

[25] GAO Y J, HUANG L L, DENG Q Q, ZHOU W Q, LUO Z R, LIN K. Phase field crystal simulation of dislocation configuration evolution in dynamic recovery in two dimensions [J]. Acta Materialia, 2016, 117: 238−251.

[26] GAO Ying-jun, DENG Qian-qian, LIU Zhe-yuan, HUANG Zong-ji, LI Yi-xuan, LUO Zhi-rong. Modes of grain growth and mechanism of dislocation reaction under applied biaxial strain: Atomistic and continuum modeling [J]. Journal of Materials Science & Technology, 2020, 49: 236−250.

[27] DUPROZ M, SUN Z, BRAND C, EWYGENHOVEN H N. Dislocation interactions at reduced strain rates in atomistic simulations of nanocrystalline Al [J]. Acta Materialia, 2018, 140: 68−79.

[28] LIU Zhi-yi, HUANG Tian-tian, LIU Wen-juan, KANG Sukbong. Dislocation mechanism for dynamic recrystallization in twin-roll casting Mg−5.51Zn−0.49Zr magnesium alloy during hot compression at different strain rates [J]. Transactions of Nonferrous Metals Society of China, 2016, 26: 378−389.

[29] MAGRI M, LEMOINE G, ADAM L, SEGURADO J. A coupled model of diffusional creep of polycrystalline solids based on climb of dislocations at grain boundaries [J]. Journal of the Mechanics and Physics of Solids, 2020, 135: 103786.

[30] FENG H, PANG J M, FANG Q H, CHEN C P, WEN P H. Enhanced ductility of nanomaterials through cooperative dislocation emission from cracks and grain boundaries [J]. International Journal of Mechanical Sciences, 2020, 179: 105652.

[31] KOSITSKI R, MORDEHAI D. Role of dislocation pile-ups in nucleation-controlled size-dependent strength of Fe nanowires [J]. Acta Materialia, 2017, 136: 190−201.

[32] GEUS De T W J, PEERLINGS R H J, HIRSCHBERGER C B. An analysis of the pile-up of infinite periodic walls of edge dislocations [J]. Mechanics Research Communications, 2013, 54: 7−13.

[33] ZHU Y C, XIANG Y, SCHULZ K. The role of dislocation pile-up in flow stress determination and strain hardening [J]. Scripta Materialia, 2016, 116: 53−56.

[34] WU M S, YU Y. Analysis of cracks nucleated by dislocation pile-ups against nonequilibrium grain boundaries [J]. Mechanics of Materials, 2000, 32: 511−529.

[35] LIU D B, HE Y M, ZHANG B, SHEN L. A continuum theory of stress gradient plasticity based on the dislocation pile-up model [J]. Acta Materialia, 2014, 80: 350−364.

[36] YUAN S L, ZHU Y X, LIANG S, HUANG M S, LI Z H. Dislocation-density based size-dependent crystal plasticity framework accounting for climb of piled up dislocations at elevated temperature [J]. Mechanics of Materials, 2019, 134: 85−97.

[37] ESHELBY J D, FRANK F C, NABARRO F R N. XLI. The equilibrium of linear arrays of dislocations [J]. The London, Edinburgh and Dublin Philosophical Magazine and Journal of Science, 1951, 42: 351−364.

[38] MARA N A, SERGUEEVA A V, MARA T D, MCFADDEN S X, MUKHERJEE A K. Superplasticity and cooperative grain boundary sliding in nanocrystalline Ni_3Al [J]. Materials Science and Engineering A, 2007, 463: 238−244.

[39] GAO Y J, HUANG L L, ZHOU W Q. Phase field crystal simulation of subgrain boundary annihilation and dislocation rotation mechanism under strain at high temperature [J]. Scientia Sinica Techologica, 2015, 45: 306−321.

[40] GAO Ying-jun, QUAN Si-long, DENG Qian-qian. Phase-field-crystal simulation of edge dislocation climbing and gliding under shear strain [J]. Acta Physica Sinica, 2015, 64: 190−200.

[41] HUANG Li-lin, GAO Ying-jun, DENG Qian-qian, LIU Zhe-yuan, LUO Zhi-rong, LI Yi-xuan, HUANG Zong-ji. A study of relationship between dislocation configuration of nanocrack and brittle-ductile mode of fracture: Atomistic modeling [J]. Computational Materials Science, 2020, 173: 109413.

[42] LIU Zhe-yuan, GAO Ying-jun, DENG Qian-qian, LI Yi-xuan, HUANG Zong-ji, LIAO Kun, LUO Zhi-rong. A nanoscale study of nucleation and propagation of Zener types cracks at dislocations: Phase field crystal model [J]. Computational Materials Science, 2020, 179: 109640.

[43] GAO Ying-jun, DENG Qian-qian, HUANG Li-lin, YE Li, WEN Zhen-chuan, LUO Zhi-rong. Atomistic modeling for mechanism of crack cleavage extension on nano-scale [J].

Computational Materials Science, 2017, 130: 64−75.
[44] DENG Qian-qian, GAO Ying-jun, LIU Zhe-yuan, HUANG Zong-ji, LI Yi-xuan, LUO Zhi-rong. Atomistic simulation of void growth by emitting dislocation pair during deformation [J]. Physica B: Condensed Matter, 2020, 578: 411767.
[45] TURTO V, RUPERT T J. Grain boundary complexions and the strength of nanocrystalline metals: Dislocation emission and propagation [J]. Acta Materialia, 2018, 151: 100−111.
[46] YUAN R, BEYERLEIN I J, ZHOU C. Grain-size effects in nanocrystallline metals from statistical activation of discrete dislocation sources [J]. Acta Materialia, 2015, 90: 169−181.
[47] KUMAR K S, SURESH S, CHISHOHM M F, HORTON J A, WANG P. Deformation of electrodeposited nanocrystalline nickel [J]. Acta Materialia, 2003, 51: 387−405.
[48] LIU Yu-shun, YAN Jia-wei, XIE Dong-yue, SHEN Yao, WANG Jian, ZHU Guo-zhen. Self-patterning screw ⟨*c*⟩ dislocations in pure Mg [J]. Scripta Materialia, 2021, 191: 86−89.
[49] TURLO V, RUPERT T J. Grain boundary complexions and the strength of nanocrystalline metals: Dislocation emission and propagation [J]. Acta Materialia, 2018, 151: 100−111.
[50] El-ATWANI O, ESQUIVEL E, AYDOGAN E, MARTINEZ E, BALDWIN J K, LI M, UBERUAGA B P, MALOY S A. Unprecedented irradiation resistance of nanocrystalline tungsten with equiaxed nanocrystalline grains to dislocation loop accumulation [J]. Acta Materialia, 2019, 165: 118−128.

晶界三叉处位错塞积的结构转变与能量分析

高英俊[1]，黄宗吉[1]，邓芊芊[1]，廖 坤[1]，李依轩[1]，易小爱[1]，罗志荣[2]

1. 广西大学 物理科学与工程技术学院，广西相对论天体物理重点实验室，广西先进能源材料重点实验室，南宁 530004；
2. 玉林师范大学 物理与电信工程学院，玉林 537000

摘 要：提出超细晶材料的三叉晶界处晶界位错塞积的结构转变能量模型。运用该能量模型，计算体系的晶界位错塞积能量，分析塞积头位错的结构转变的临界几何条件和力学条件，讨论塞积位错的数密度和三叉晶界处的二个分解位错 Burgers 矢量之间的角度对头位错转变模式的影响。结果表明，当晶界位错在三叉晶界处塞积，只要这二个位错 Burgers 矢量夹角小于 90°，头位错就能够分解为二个新的位错；外加应力的增加能够减少位错分解的阻力。另外，还揭示出超细晶材料同时具有高的强度和塑性的机理，归因于三叉晶界处的塞积位错的结构转变。

关键词：晶界三叉点；位错塞积；位错结构转变；塞积能量模型；超细晶材料

(Edited by Bing YANG)